analytical chemistry

ARTICLE

pubs.acs.org/ac

Microfabricated Gas Chromatograph for the Selective Determination of Trichloroethylene Vapor at Sub-Parts-Per-Billion Concentrations in Complex Mixtures

Sun Kyu Kim,[†,‡] Hungwei Chang,[†,‡] and Edward T. Zellers*[,†,‡,§]

[†]Department of Environmental Health Sciences, University of Michigan, Ann Arbor, Michigan 48109-2029, United States

[‡]Center for Wireless Integrated MicroSystems, University of Michigan, Ann Arbor, Michigan 48109-2122, United States

[§]Department of Chemistry, University of Michigan, Ann Arbor, Michigan 48109-1055, United States

Supporting Information

ABSTRACT: A complete field-deployable microfabricated gas chromatograph (μGC) is described, and its adaptation to the analysis of low- and subparts-per-billion (ppb) concentrations of trichloroethylene (TCE) vapors in complex mixtures is demonstrated through laboratory testing. The specific application being addressed concerns the problem of indoor air contamination by TCE vapor intrusion. The μGC prototype employs a microfabricated focuser, dual microfabricated separation columns, and a microsensor array. These are interfaced to a nonmicrofabricated front-end pretrap and high-volume sampler module to reduce analysis time and limits of detection (LOD). Selective preconcentration and focusing are coupled with rapid chromatographic separation and multisensor detection for the determination of TCE in the presence of up to 45 interferences. Autonomous operation is possible via a laptop computer. Preconcentration factors as high as 500 000 are achieved. Sensitivities are constant over the range of captured TCE masses tested (i.e., 9−390 ng), and TCE is measured in a test atmosphere at 120 parts-per-trillion (ppt), with a projected LOD of 40 ppt (4.2 ng captured, 20 L sample) and a maximum sampling + analytical cycle time of 36 min. Short- and medium-term (1 month) variations in retention time, absolute responses, and response patterns are within acceptable limits.

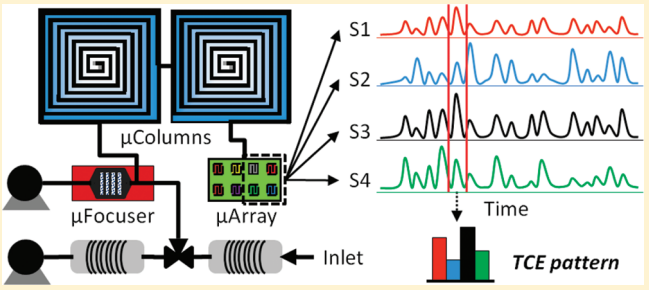

Gas chromatographic microsystems (μGC) fabricated using Si-micromachining batch processing techniques have been the subject of a resurgence of interest over the past decade and represent perhaps the most promising technology for meeting the need for small, low-power field instruments capable of analyzing volatile organic compounds (VOC) in moderately complex mixtures. Some prominent target applications include ambient air monitoring, worker exposure assessment, military surveillance, homeland security, and biomedical diagnostics.

Most of the research on μGC over this period of time has focused on the individual components of such microsystems, including micropumps,[1] micropreconcentrators,[2] microcolumns,[3] and microsensor or microsensor-array detectors.[4] Several reports have described subsystems that combine a microcolumn with one other microscale component.[3k,5,6] However, only a handful of studies have addressed complete μGC systems,[7] defined here as comprising a fluidically interconnected ensemble of at least the following three essential components, all of which are microfabricated: a preconcentrator or other injector, a separation column, and a detector. The small number of such reports attests to the challenges associated with microsystem integration.

Among the earliest of these was a series of reports on a laboratory prototype μGC produced in our laboratory, which was capable of determining the components of moderately complex VOC mixtures at parts-per-billion (ppb) concentrations.[7a−c] It included a multistage microfabricated preconcentrator/focuser (μPCF), which served as both a trap and an injector, a microcolumn with a 3 m-long separation channel, and a detector consisting of an integrated array of four chemiresistors (CR) that employed thiolate-monolayer-protected gold nanoparticles (MPN) as the sorptive interface layers. Performance trade-offs were explored as a function of several operating variables. Combining the response pattern generated from the microsensor array with the corresponding chromatographic retention time facilitated the differentiation and identification of the components of the 11-VOC mixture that was analyzed.[7c] Since then, in collaboration with our colleagues,[8] we have improved the design and performance of several of the original μGC components,[3k,4l,4n,4o,9,10] developed new components,[11−14] and made further progress toward integrating them into microsystems for the quantitative analysis of VOC mixtures.[3k,6,7f,7h,7i,15,16]

Received: July 11, 2011
Accepted: August 4, 2011
Published: August 22, 2011

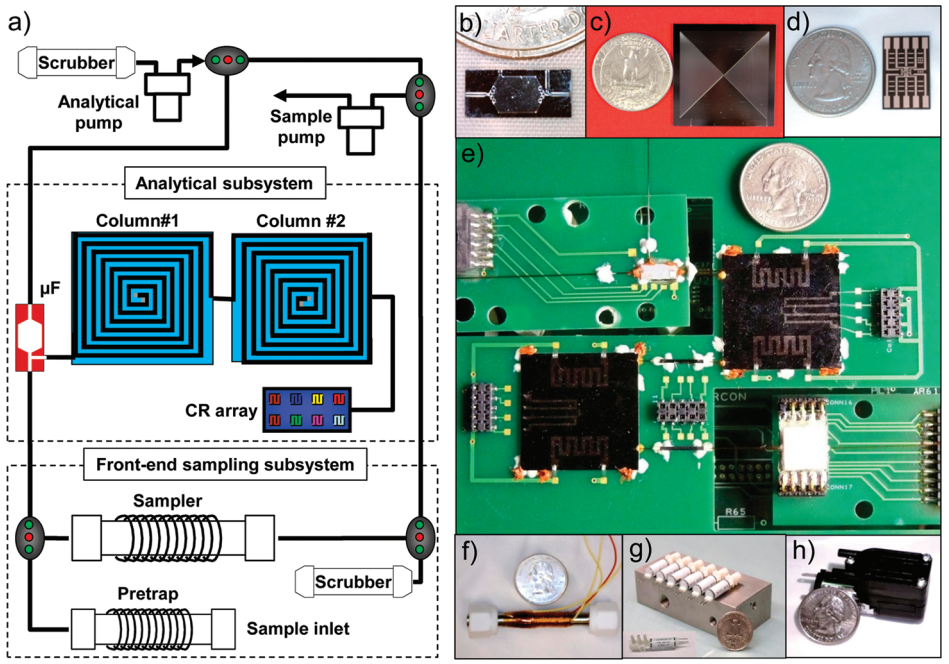

Figure 1. Fluidic pathway diagram of the μGC prototype and photographs of the major components: (a) schematic diagram showing fluidic pathways; (b) microfocuser (μF); (c) 3 m microcolumn; (d) microsensor array; (e) integrated microanalytical subsystem; (f) high-volume sampler/pretrap; (g) valve and valve manifold; (h) miniature diaphragm pump.

The specific application for which the prototype described here has been optimized concerns the measurement of trichloroethylene (TCE) vapors arising from a phenomenon called vapor intrusion (VI). VI refers to indoor air contamination arising from the migration of VOCs into occupied structures from underlying contaminated soil or groundwater.[17] TCE is a common soil contaminant found in proximity to numerous hazardous waste sites around the U.S. due to its historically widespread use as a degreasing solvent, indiscriminant disposal, environmental persistence, and volatility.[18] Indoor air concentrations of TCE arising from VI are often in the low- or subppb range,[19−21] which is also the range within which many common indoor air contaminants are typically encountered.[22] Therefore, determining TCE in locations potentially affected by VI requires preconcentration and separation from such cocontaminants.

Among the few currently available direct-reading instruments capable of *in situ* determinations of TCE at such low concentrations in the presence of numerous possible cocontaminants, the portable GC/MS appears to be the most effective due to its combination of chromatographic separation and spectrometric detection.[23,24] However, the utility of GC/MS for continuous, long-term assessments of indoor air contamination in multiple locations is severely limited by its cost and operating complexity. Thus, there remains a need for portable instruments capable of determining trace levels of specific VOCs in complex mixtures, yet small, simple, and inexpensive enough to be used for routine monitoring.

In this Article, we describe the design, development, assembly, and laboratory characterization of a high-performance μGC field prototype adapted specifically for TCE determinations in VI-impacted homes. An overview of the key components of the system as well as the application-specific variables that dictated their design, configuration, and operating conditions are provided in the next section. Descriptions of the materials, methods, and components used, along with their physical and functional integration are then provided, followed by results demonstrating the performance of the assembled prototype.

Analytical Subsystem Design and Operating Conditions. Figure 1a shows a schematic diagram of the primary analytical components and fluidic pathways of the instrument. A commercial mini-pump (sample pump) draws an air sample through the manifold-mounted pretrap and sampler at a high flow rate, bypassing the other components. Then, the appropriate valves are actuated, and the sample pump draws scrubbed ambient air in the opposite direction through the sampler as it is resistively heated and backflushed to desorb and transfer the captured VOCs (including TCE) to the microfocuser (μF) at a lower flow rate. Following another set of valve actuations, the analytical mini-pump draws scrubbed air in and pushes it through the μF as the μF is heated rapidly to backflush and inject the captured VOC mixture into the first of two series-coupled microcolumns for analyte separation and detection by the array of nanoparticle-coated CR microsensors.

This laboratory study was performed in preparation for field testing in several residences near a U.S. Air Force base where TCE VI has been documented.[25] An indoor air concentration of 2.3 ppb was established as a "mitigation action level" (MAL) for homes near this site, and historical monitoring indicated that TCE concentrations were most commonly between 0.2 and 8 ppb. On this basis, we established a target limit of detection (LOD) of 0.06 ppb, a corresponding limit of quantitation of 0.2 ppb, and a calibration concentration range of ~40-fold for the prototype. Preliminary testing with the CR array detector installed downstream from the microcolumns yielded a provisional LOD for TCE of 1.2 ppb from a 1 L preconcentrated air sample.[7h] This corresponds to an integrated volume of 1.2 ppb-L and a mass of 6.4 ng of captured TCE. Therefore, a sample volume of 20 L would be required to detect 0.06 ppb of TCE.

Our previous work with μPCFs[2b,c,7c] and other miniaturized preconcentrators[4b,26] suggested that such a large air sample volume would likely result in some degree of breakthrough of TCE, even at the low concentrations expected in the field. The narrow cross section and small volume of this device would also limit the maximum volumetric flow rates that could be passed through it, which would lead to excessively long sampling periods. In addition, any semivolatile organic compounds present in the air would be expected to adsorb strongly to all exposed surfaces and only slowly desorb from the μPCF at normal desorption temperatures.[4k,4q] Furthermore, the finite peak capacity of the relatively short microcolumns employed would limit the capability to chromatographically separate TCE from cocontaminants in captured samples.

To address this set of constraints, we developed a front-end preconcentrator-focuser (PCF) module consisting of a pretrap of conventional design (i.e., an adsorbent-packed metal tube) for capturing interferences with vapor pressures (p_v) < 3 Torr and a high-volume sampler, also of conventional design, for capturing (and transferring) TCE and other compounds with p_v values within the range of ~3−95 Torr. Compounds with higher p_v values are allowed to pass through largely unretained. The sampler then transfers the captured VOCs to the μF chip for focusing and injection into the separation module. This PCF module provides the means to selectively and quantitatively capture, transfer, and inject TCE vapor samples at the required concentrations in the presence of common indoor air contaminants.[10] It also greatly reduces the time required for a complete sampling and analysis cycle; although somewhat arbitrary, a target of roughly two measurements per hour was set to provide a level of temporal resolution sufficient for guiding assessment and remediation efforts in the field.

Prior tests with the two 3 m microcolumns, both wall-coated with a polydimethylsiloxane (PDMS) stationary phase, indicated that ~3 min would be required for TCE and the most common cocontaminants that might be captured and injected along with TCE to elute with good chromatographic resolution.[7i] An estimate of the number of theoretical plates, N, required for such separations under the analytical conditions employed is consistent with this finding (see Supporting Information). Allowing a few minutes for the focusing step and for subsequent sensor baseline stabilization prior to injection, a sampling flow rate of ~1 L·min^{-1} was determined to be sufficient to meet the overall analysis time limit of ~30−40 min for samples requiring the maximum anticipated volume of 20 L.

EXPERIMENTAL METHODS

Materials. The compounds used as potential interferences are a subset of the 63 VOCs found (by GC/MS) in a series of 12 air samples collected from VI-impacted residences near the site where field tests were ultimately conducted. These ranged in p_v values from 0.085 to >5000 Torr. Since most of the 27 detected compounds with p_v values >100 Torr are (by design) not captured efficiently by the adsorbent in the sampler, all but a few of them were eliminated from the test set. Some of the moderate- and low-volatility compounds were replaced with other compounds of similar structure and volatility often found as contaminants in indoor air that were available in the laboratory. The resulting set of 45 cocontaminants, which was considered sufficient to demonstrate selective TCE determinations, is presented in Table S1 in the Supporting Information.

All VOCs were purchased from Sigma-Aldrich/Fluka (Milwaulkee, WI) or Acros/Fisher (Pittsburgh, PA) in >95% (most >99%) purity and were used as received. The adsorbents used were graphitized carbons obtained from Supelco (Bellefonte, PA): Carbopack B (C-B, specific surface area = 100 m^2/g) was used in the pretrap and Carbopack X (C-X, 250 m^2/g) was used in the sampler and the μF. Samples of C-B and C-X (60/80 mesh) were sieved, and the fractions with nominal diameters in the range of 212−250 μm were isolated and packed in the appropriate device. The PDMS stationary phase polymer was obtained from Ohio Valley (OV-1, Marietta, OH), and the surface pretreatment agent hexamethyldisilazane (HMDS) was obtained from Acros Organics (Geel, Belgium). MPNs derived from the following thiols were taken from existing supplies that were synthesized by the method reported by Rowe et al.:[27] *n*-octanethiol (C8), 6-phenoxyhexane-1-thiol (OPH), 4-(phenylethynyl)-benzenethiol (DPA), and methyl-6-mercaptohexanoate (HME). The MPNs had core diameters in the range of 3.4−4.7 nm.[4n]

PCF Module Components. The pretrap and sampler were constructed from thin-walled stainless-steel tubes (0.64 cm o.d.; 0.54 cm i.d.; 6 cm long). A 50 mg bed of C-B was used in the pretrap, and a 100 mg bed of C-X was used in the sampler. The pretrap does not retain TCE, and the 10% breakthrough volume of TCE through the sampler at 1 L·min^{-1} is >30 L in the presence of 23 interferences (each at ~50 ppb) at high humidity.[10] Both devices were heated with coils of insulated Cu wire and monitored with thermocouples held snugly against the tube walls by the Cu coils.

The μF chip has dimensions of 9.76 × 4.18 × 0.6 mm. Deep-reactive-ion-etching (DRIE) was used to form a 3.2 (w) × 3.45 (l) × 0.38 mm (h) cavity with additional tapered sections leading to the inlet and outlet ports at opposing ends of the Si substrate, a set of pillars near the inlet and outlet ports to retain the adsorbent within the cavity, and inlet and outlet channels one of which has a right-angle tee-branch. The device was capped with an anodically bonded Pyrex plate. Cr/Au contact pads were evaporated onto the backside of the substrate for bulk resistive heating, and a Ti/Pt resistive temperature device (RTD) was patterned near the contacts for monitoring temperature. C-X (~2.3 mg) was loaded into the μF using gentle suction. Deactivated fused-silica interconnection capillaries (0.25 mm i.d., 0.32 mm o.d., Restek Corp., Belafonte, PA) were secured with adhesive (Duraseal 1531, Cotronics, Brooklyn, N.Y). Electrical connections to a custom printed circuit board (PCB) were made via Al wire bonds.

The maximum μF desorption temperature of 225 °C employed was sufficient to desorb TCE rapidly and completely, while low enough to minimize the risk of thermal degradation of the C-X, which we have found to shed small particles after repeated thermal cycling at >250 °C in air. During injection, the μF was heated at 440 °C/s for 0.45 s, maintained between 225 and 250 °C for 120 s, and then allowed to cool. (See Figure S1 in the Supporting Information for a representative heating profile.)

Microcolumns. Each microcolumn chip has a 3 × 3 cm footprint and comprises a convolved square-spiral channel 3 m long with a rectangular cross section, 150 × 240 μm, formed in Si by DRIE and sealed by an anodically bonded Pyrex cover plate.[3f,l] The peripheral inlet and outlet ports accommodate deactivated fused-silica capillaries (250 μm i.d.) that were sealed with epoxy (Hysol Epoxy Patch 1C, Henkel Corp., Rocky Hill, CT). Two meander-line Cr/Au heaters and a Ti/Pt RTD evaporated onto the backside of the microcolumns were used for programmed

heating during separations. In this study, one set of microcolumns was modified by chamfering the corners within the spiral using a different DRIE mask during fabrication and enlarging the heaters to improve the heat-transfer efficiency and uniformity. The microcolumns were individually pretreated with HMDS, coated with a PDMS stationary phase from solution using a static deposition method, and then cross-linked using dicumyl peroxide (calc. avg. film thickness = 0.15 μm).[3l]

The maximum N produced by the microcolumns with chamfered corners is 4550 plates/m, which is ~20% greater than that produced from microcolumns with right-angle corners. (See Supporting Information for Golay plots, experimental details, and a representative chromatogram.) For all separations, microcolumn temperatures were maintained at ≤120 °C to minimize stationary phase bleed.[4l]

Chemiresistor (CR) Array. Responses from MPN-coated CRs derive from the swelling induced changes in interparticle distance as well as any changes in the dielectric constant accompanying reversible vapor sorption.[4f] The CR array used in the prototype is the same as that used in a mesoscale instrument reported on previously.[4j,25] The array chip has dimensions of 2.0 × 1.2 cm and consists of 8 Au/Cr interdigital electrodes (IDEs) deposited in a 4 × 2 pattern on a thermal-SiO_x/Si substrate. Each IDE has 24 finger pairs (5 μm widths/spaces, 450 μm length, 410 μm overlap). A Macor lid with inlet/outlet ports was sealed to the substrate using a gasket of VHB tape (3M, St. Paul, MN) to create a detector cell volume of 1.6 μL (0.3 (w) × 0.4 (l) × 0.013 cm (h)). Deactivated fused-silica capillaries were sealed into the ports with Hysol epoxy. Two sensors were coated with each type of MPN by drop casting from solution with a 0.5 μL syringe to create multilayer films with baseline resistances within the range of 1−10 MΩ. (Note: thicknesses were not determined.) The CR array temperature was monitored via a calibrated on-chip RTD.

Device Mounting and System Integration. The assembled prototype has dimensions of 44 (w) × 25.5 (d) × 14.5 cm (h) and weighs 4.5 kg. Photographs of the key fluidic and analytical components are provided in Figure 1b−h. A stainless-steel manifold was created with top-surface access ports designed to match those on each of six 3-way latching microsolenoid valves (Lee Co., Westbrook, CT) which were bolted in place (Figure 1g). The pretrap and sampler were also mounted on the manifold using Teflon Swagelok fittings tapped into opposing sidewalls (Figure 1f,g). The two miniature diaphragm pumps (NMS020, KNF Neuburger, Trenton, NJ; Figure 1h) were located beside the manifold and connected to the appropriate ports via flexible tubing.

The μF, CR array, and the dual-microcolumn separation module (Figure 1b−e) were mounted and wire-bonded on separate carrier PCBs which, in turn, were mounted on standoffs to the floor of the prototype. Cut-outs in the microcolumn PCB reduced the distances among these devices, which were connected by use of glass press-fits (Agilent Technologies, Palo Alto, CA). Two large, cylindrical scrubbers (Restek), each containing Drierite and 5 Å molecular sieves, as well as two smaller scrubbers containing activated charcoal (SKC Inc., Eighty Four, PA), were mounted to the external walls of the prototype chassis and used to remove water vapor and background organic vapors, respectively, during focusing and analysis. Additional components included two power supplies and three cooling fans. The custom circuit boards and associated DAQ cards used to monitor and control the prototype components are described in the Supporting Information.

Device Control and System Operation. Each measurement cycle consisted of sampling, focusing, stabilization, and analysis steps. User-defined pump, valve, and heater actuation timing and temperature settings, as well as the temperature program for each microcolumn, could be entered at the start of a run through the graphic user interface of the custom instrument control program written in LabView and automatically implemented. However, manual operation of each step was also possible and was often used during testing. The timetable for a typical operating cycle as well as a summary of the power requirements are presented in the Supporting Information.

The sampler and pretrap were preconditioned at 300 °C for 30 min under N_2 before initial use and were periodically heated with backflushing under N_2 thereafter to remove residual trapped VOCs. VOCs were desorbed from the sampler to the μF at 220 °C by application of a constant dc voltage bias to the heater coil. The μF was heated to 225 °C by the application of a high initial dc voltage bias followed by a lower maintenance voltage. The microcolumns were temperature programmed using a pulse-width-modulation method with a proportional-integral-derivative algorithm incorporated into a LabView subroutine. Up to six settings and ramp rates could be specified for each microcolumn in a given run.

Resistance changes of the CR sensors were measured indirectly by applying a constant dc voltage to each CR through a 1 MΩ reference resistor, forming a voltage divider. The voltage drop across each CR was recorded by the DAQ card at 20 Hz after amplification of the signal difference between baseline and measured values. The methods used for data analysis and subsequent chemometric analysis are described in the Supporting Information.

Test-Atmosphere Generation. Test atmospheres of TCE were generated by diluting samples taken from a certified compressed gas cylinder (Scott Specialty Gases Inc., Troy, MI) containing TCE vapor at either 11 or 20 ppb (in N_2) with N_2 in Tedlar bags. For certain tests, concentrations of the test atmospheres were confirmed by collecting samples in Summa canisters and analyzing by GC/MS according to EPA Method TO-15[28] (analyses performed by Columbia Analytical Services, Simi Valley, CA). For tests run with other VOC interferences, a small volume (2.5 to 30 μL, depending on the compound) of headspace from a vial of each pure liquid was drawn into a gastight syringe and injected on a background of clean air into the system through the septum port in a temporary tee connector placed in line upstream from the inlet.

RESULTS AND DISCUSSION

System Integration. Due to unanticipated flow restrictions attributable to several narrow-bore passages within the valve manifold, the maximum flow rate achievable during sampling was 0.78 L·min^{-1}. Therefore, collecting the largest anticipated sample volume of 20 L required 26 min. Focusing at 18 mL·min^{-1} for 3 min was sufficient to transfer TCE quantitatively to the μF (i.e., subsequent blank analyses yielded no measurable TCE) without breakthrough of the μF adsorbent bed.[10] For the stabilization step, the flow through the microcolumns and sensor array was set at 1.2 mL·min^{-1} (discussed immediately below) and a minimum period of 3 min was required in order to regain stable sensor baseline signals. Although it required <1 min for TCE to elute during the analysis step, up to 3.5 min was allowed for elution of the remaining mixture components to illustrate

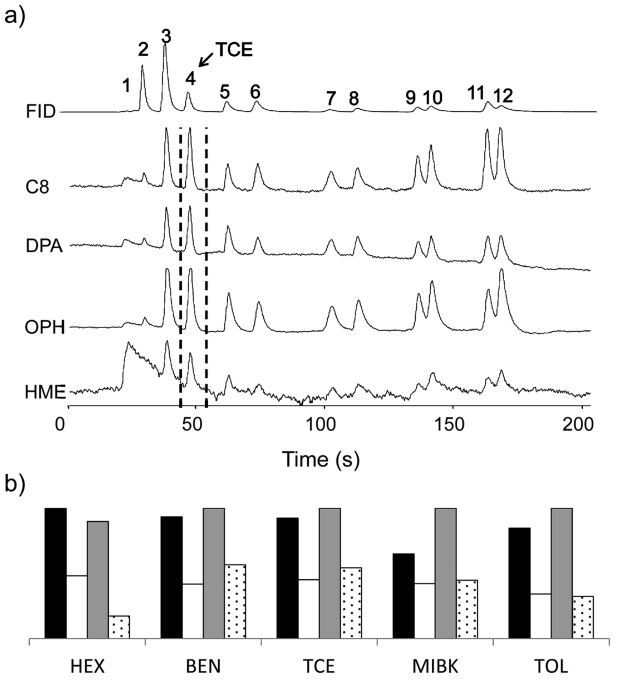

Figure 2. (a) 3-minute chromatograms from the four CR microsensors and a downstream FID generated from the analysis of a 20 L air sample spiked with TCE and 11 VOC interferences by the μGC prototype. Peak assignments are as follows: 1, 2-propanol; 2, *n*-hexane (HEX); 3, benzene (BEN); 4, TCE; 5, 4-methyl-2-pentanone (MIBK); 6, toluene (TOL); 7, perchloroethylene; 8, butylacetate; 9, ethylbenzene; 10, *m*-xylene; 11, nonane; 12, cumene. The mixture composition was adjusted so that the range of sampled masses (34−1700 ng) decreased with decreasing analyte volatility (increasing retention time) and peaks of comparable size were obtained for all components in the chromatograms. Temperature program of 1st microcolumn: hold at 25 °C for 40 s, heat to 50 °C at 1.25 °C/s, heat to 120 °C at 0.58 °C/s, hold at 120 °C for 60 s. Temperature program of 2nd microcolumn: hold at 25 °C for 45 s, heat to 60 °C at 0.64 °C/s, heat to 120 °C at 0.75 °C/s, hold at 120 °C for 60 s. (b) Normalized CR array response patterns for TCE and proximate interferences (black: C8, white: DPA, gray: OPH, dotted filled: HME).

their full or partial resolution. (Note: this time period could be reduced by increasing the rate of heating.) Thus, the maximum total sampling and analytical cycle time was ∼36 min.

Reconciling flow rates among the devices in the analytical subsystem required trade-offs in the various aspects of performance.[7b] Previous work had shown that the injection bandwidth of TCE from the μF decreased sharply between 0.2 and 1 mL·min^{-1} and then more gradually up to 2 mL·min^{-1}, reaching a minimum full-width-at-half-maximum (fwhm) value of 1s by FID.[10] Although the optimal efficiency for the dual column ensemble occurs at 0.22 mL·min^{-1} in air or N_2, the fwhm of the injection band at this low flow rate is >2.7 s, which precludes the separation of TCE from early eluting cocontaminants. Increasing the flow rate to 2 mL·min^{-1} minimizes the injection bandwidth but also decreases *N* from 4500 to ∼700 plates/meter. The peak areas and fwhm values from the CR sensors have been shown to decrease sharply up to a flow rate of 1.0 mL·min^{-1}, followed by a more gradual decrease up to 3.3 mL·min^{-1}.[4k] Thus, although lower flow rates yield higher sensitivities, they also yield broader peaks and incur a very high *sensitivity* to flow rate, which are undesirable. Notably, peak height shows a much smaller dependence on flow rate, which argues for the use of peak height as the sensitivity parameter.[4k] The analytical flow rate of 1.2 mL·min^{-1} adopted for all subsequent testing represents a compromise among the efficiency, resolution, speed, and sensitivity of the analysis.

Chromatographic Resolution and Array Response Patterns. A subset of 11 VOCs with p_v values ranging from 3.5 to 150 Torr, bracketing that of TCE (p_v = 69 Torr), was selected to develop the separation conditions and to illustrate the performance of the prototype. The set of chromatograms in Figure 2a was generated from the analysis of a 20 L spiked air sample with the prototype. As shown, TCE was separated from the 11 interferences in 45 s and the entire mixture eluted in <3 min. The temperature program used for each microcolumn was determined empirically. A more aggressive heating ramp (i.e., > 7.6 °C·s^{-1}) could be implemented after the first 45 s to reduce the analysis time, with a consequent loss of resolution of the later eluting compounds. This particular separation did not require the more elaborate temperature programming capability built in to the instrument.

The chromatogram from the HME-coated sensor shows an exceptionally large artifact peak at a retention time of ∼25 s with a long tail that overlaps the TCE peak. This was eventually determined to be due to water vapor drawn into the system during focusing by a small leak in the downstream Teflon fitting of the sampler. Separate testing confirmed that the water sensitivity of the HME sensor is significantly greater than that of the other sensors in the array, consistent with the data shown in Figure 2a. Despite the overlap with the tail of this peak, it was possible to obtain sensitive and reproducible TCE responses from the HME sensor.

The mixture component eluting most closely to TCE is benzene. For the measured retention time (t_R) values of 39.1 and 45.3 s and fwhm values of 2.1 ± 0.3 and 2.0 ± 0.2 s (among all 4 sensors) for benzene and TCE, respectively, the resolution is 1.7. This is comparable to the resolution provided by the FID (top trace in Figure 2a); however, since the latter was placed downstream from the CR array, it was subject to the band broadening associated with the array detector cell and interconnecting capillary (∼40 cm). Regardless, it is interesting to note the differences in the relative magnitudes of various peaks between the sensors and the FID. For example, the benzene/TCE peak area ratio of 3.9 for the FID reflects the low sensitivity of the FID to chlorinated hydrocarbons, whereas the ratio of 1.1 for the C8 sensor (similar to the other sensors) reflects the similarity in partition coefficients of the two vapors in the MPN films.[4n]

CR array response patterns are presented in Figure 2b for TCE and the subset of four compounds eluting most closely to TCE. The TCE response pattern is quite distinct from those of *n*-hexane and MIBK but rather similar those of benzene and toluene, consistent with previous reports of microsensor arrays employing polymer or MPN interface layers.[4p,q] To assess the ability to recognize TCE and differentiate it from the other vapors in the set on the basis of its response pattern, retention time notwithstanding, Monte Carlo simulations coupled with EDPCR analyses were performed with the relative response patterns generated from the data in Figure 2b. Details of the methodology and the resulting confusion matrix are presented in the Supporting Information.

For TCE, the recognition rate (RR) value is only 80%, with the error being due almost entirely to confusion with benzene

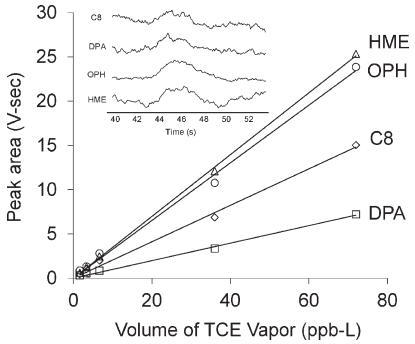

Figure 3. Calibration curves generated from sampling different volumes of test atmospheres of TCE in air. The net TCE volumes ranged from 1.7 to 72 ppb-L (9−390 ng): linear regression (forced zero) r^2 values are all >0.99. Concentrations were confirmed by independent GC/MS analysis. Inset shows chromatograms from the analysis of a test atmosphere containing 0.12 ppb of TCE in air (sample volume: 20 L; TCE volume: 2.4 ppb-L; TCE mass: 13 ng).

Table 1. Limits of Detection for TCE from Each Sensor in the Array for Two Assumed Sample Volumes

	LOD[a] (ppb)	
sensor	1 L	20 L
C8	1.7	0.08
DPA	2.4	0.12
OPH	0.8	0.04
HME	1.4	0.07

[a] LOD = 3s/sensitivity, where s = standard deviation of baseline noise determined for each sensor and sensitivity was taken as the slope of the calibration curve in Figure 3.

(i.e., excluding benzene, the RR value for TCE is >99.5%). The RR values for *n*-hexane, benzene, MIBK, and toluene are 100, 83, 99, and 99%, respectively. The low value for benzene is due to its confusion with TCE. Thus, while this confirms the value of the CR array to help identify TCE (and other analytes), it also emphasizes the need for chromatographic separation in utilizing the CR array (or any other microsensor array) for multivapor analyses.

Calibration, Detection Limits, and Accuracy. Figure 3 shows a set of calibration curves for TCE obtained by collecting samples of different volumes from two test atmospheres generated in Tedlar bags from a compressed gas cylinder containing a low TCE concentration. The TCE bag concentrations were found to be 0.83 and 18 ppb from duplicate canister samples analyzed by GC/MS. Ambient temperature and relative humidity during testing were 25 °C and 20%, respectively. Sample volumes of 2−8 L were collected and analyzed, resulting in a range of captured TCE masses from 9 to 390 ng and integrated vapor volumes of 1.7−72 ppb-L.

As shown, responses (peak areas) vary linearly with concentration. The corresponding plots of peak height show similar relative sensitivities and the same degree of linearity. TCE LODs calculated on the basis of these data are presented in Table 1 for assumed sample volumes of 1 and 20 L. For the latter, the LODs range from 0.04 ppb (OPH) to 0.12 ppb (DPA). For reference, single-point estimates of the sensitivities for a subset of other vapors from Figure 2a were used to derive rough estimates of their LODs, as well: using the sensor that provided the lowest LOD value in the array for a given vapor, these range from 0.010 ppb for *m*-xylene (OPH) to 15 ppb for 2-propanol (C8) assuming a 20 L sample. (Note: *n*-nonane and cumene were excluded because of significant retention by the pretrap, which also occurs to a lesser extent for other compounds eluting after TCE.)

Table 2. Short- and Medium-Term Stability of Retention Times and Sensor Responses

		RSD (%)[a]		
period	sensor	peak area	peak height	t_R
short-term[b]	C8	9.1	8.1	0.9
	DPA	3.9	2.7	1.0
	OPH	3.7	2.2	0.9
	HME	5.6	9.5	0.9
	avg	5.6	5.6	1.0
medium-term[c]	C8	8.2	9.5	1.4
	DPA	15	13	1.4
	OPH	10	7.7	1.3
	HME	10	9.4	1.4
	avg	11	9.9	1.4

[a] Relative standard deviation. [b] n = 10 replicates within a single day. [c] n = 15 replicates over 1 month.

The inset of Figure 3 shows the raw response data from all four sensors for a 20 L sample collected from a test atmosphere containing 0.12 ppb TCE (confirmed by GC/MS). Using the aforementioned calibration data, the average value obtained with the prototype using the peak areas from the four sensors was 0.12 ± 0.033 ppb (0% error) and that using peak heights was 0.14 ± 0.035 ppb (+17% error). An additional 4 L sample of a test atmosphere containing 11 ppb of TCE (also confirmed by GC/MS) gave an average of 11 ± 0.40 ppb (0%error) on the basis of the peak area calibrations and 12 ± 0.70 ppb (+9% error) on the basis of peak height. This degree of accuracy is sufficient for the intended purpose.

The preconcentration factor (PF) achieved by use of the high-volume sampler can be evaluated by taking the ratio of the sample volume to the volume of the peak measured at the detector, assuming that the same mass of TCE is contained in both (i.e., that the transfer efficiency is 100%). This corresponds to the ratio of the atmospheric concentration to the concentration delivered to the sensor array. For a fwhm value of 2.0 s at 1.2 mL·min^{-1} (0.02 mL·s^{-1}), the volume of the TCE peak is ∼0.04 mL. For a 20 L sample volume, PF = 500 000.

Stability. Previous reports have noted that the responses from MPN-coated CR sensors can drift over time, often significantly.[4k,o] The short-term stabilities of the retention times, responses, and response patterns were examined by replicate analyses of 2 L samples of 11 ppb of TCE (n = 10). Results are summarized in Table 2. The retention times varied by <1% (RSD) for all 4 sensors (t_R = 45.3 s), and the variation in peak areas ranged from 3.7% (OPH) to 9.1% (C8) (avg = 6.1%) for signal-to-noise ratios ranging from 25 (C8) to 94 (OPH). Similar results were obtained when peak height values were used.

The stability of the response pattern was assessed using the pairwise correlation coefficients (r) between the pattern for the first sample and those of each subsequent sample. The r values ranged from 0.97 to 1.00 (peak area or height) for the first nine replicates and decreased to 0.95 for the last sample due to an anomalously low response from the HME sensor. Another set of

dx.doi.org/10.1021/ac201788q |*Anal. Chem.* 2011, 83, 7198–7206

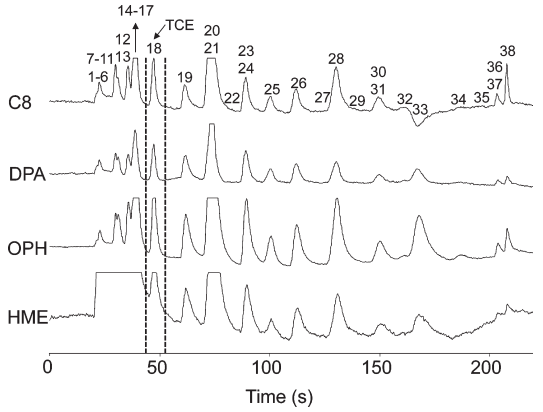

Figure 4. Chromatograms from the four CR microsensors generated from the analysis of a 20 L air sample spiked with TCE and 45 interferences. Eight of the interferences were (by design) retained by the pretrap and therefore do not appear in the chromatograms. Numbers correspond to the compounds listed in Table S1 of the Supporting Information.

replicates (n = 6) collected for mixtures of benzene, toluene, ethylbenzene, and m-xylene spiked into each 20 L air sample gave RSDs of 0.4−0.9% and 13−30% (avg = 23%) for retention time and peak height, respectively. The relatively large variation in peak height values is attributed to the use of manual (syringe) injections to spike the air samples and to partial retention of the latter three compounds on the pretrap adsorbent.

Medium-term stability was also examined by analyzing replicate 2 L samples of 11 ppb of TCE every few days for 4 weeks (Table 2). Within a given day, the RSD values among the responses (peak heights) from all sensors (n = 4) were <9.3% and averaged 6.6% over the 15 days on which tests were run. Over the month, the RSDs of the grand averages of the 15 daily (average) values ranged from 7.7% (OPH) to 13% (DPA) among the four sensors. The largest amount of drift was observed over the first week, after which sensitivities changed by <10%. Net drifts ranged from −26 to +15% of the starting sensitivity values. Accordingly, the pairwise correlations between the relative response pattern for TCE from the first day and those from subsequent samples decreased over the first week (i.e., from r = 1.00 to 0.95) but then stabilized over the subsequent 3 weeks (i.e., r > 0.99). (Note: drift of a similar magnitude is apparent between the TCE responses in Figures 2 and 3, which were collected 2 weeks apart.)

Complex Mixture Analysis. To test the ability of the prototype to analyze TCE in the presence of a large number of interferences, a mixture of 46 VOCs was introduced on a background of 20 L of clean air. Focusing, separation, and detection proceeded as described above, and the microcolumn temperature programs were the same as those used to generate the chromatograms in Figure 2a. Figure 4 shows the traces with each of the 38 other compounds not (completely) retained in the pretrap designated by number. Eight of the 10 compounds with p_v values <3 Torr were effectively captured by the pretrap, while two broke through to the sampler and were focused and analyzed. As shown, TCE is completely resolved and elutes in 45 s, and the entire mixture elutes within ∼3.5 min. The tailing peak seen in the HME-sensor trace is a combination of water vapor (primarily) and a few of the more volatile, polar interferences to which the (polar) HME MPN has the most affinity.

Notably, benzene, toluene, ethylbenzene, and m-xylene are also resolved in this analysis, which suggests that they could be analyzed effectively with the prototype, following some modifications to the pretrap to ensure that they are transferred from the atmosphere to the sampler quantitatively. This bodes well for adapting the prototype to the quantitative analysis of multiple target compounds in the vapor pressure range of ∼3−95 Torr.

CONCLUSIONS

This is the first report of a field-deployable μGC prototype employing microsensor array detection for environmental monitoring that is capable of selective multi-VOC determinations at subppb concentrations. Optimized for TCE, the instrument relies on selective high-volume preconcentration; microfocuser injection; rapid, temperature-programmed, dual-microcolumn separation; and microsensor-array recognition and quantification to analyze TCE in the presence of a complex mixture of background VOCs. The sensitivity, selectivity, accuracy, stability, and sampling + analytical cycle time demonstrated here, coupled with the capability for automated operation, indicate that this type of instrument would be effective in guiding efforts to monitor and mitigate TCE vapor intrusion in affected residences. In addition, it appears feasible to extend its use to the simultaneous analysis of other VOCs at subppb concentrations, such as benzene, toluene, ethylbenzene, and xylene.

All of the analytical components of this μGC were microfabricated using standard processing methods and materials, which affords several inherent advantages, including: simple, high-yield, modular (interchangeable) components; small fluidic path dimensions and low dead volumes; rapid, low-power heating (for the μF and microcolumns); and low-profile multidimensional (spectrometric) detection. However, this study revealed that the collective demands of the specific application addressed here, i.e., quantitative analysis of a relatively volatile target vapor at trace-level concentrations in the presence of numerous cocontaminants in a short period of time, could not be met by the microsystem alone and required the use of a (selective) front-end preconcentration module made from nonmicrofabricated components.

Since completing this study, we have deployed two prototypes of this design in the field for tests in a home impacted by TCE arising from vapor intrusion. Results of these studies, which demonstrate the use of these instruments for monitoring spatial and temporal variations in TCE concentrations, will be reported in the near future.

ASSOCIATED CONTENT

Supporting Information. Additional data and explanatory text. This material is available free of charge via the Internet at http://pubs.acs.org.

AUTHOR INFORMATION

Corresponding Author
*E-mail: ezellers@umich.edu.

ACKNOWLEDGMENT

The first two authors contributed equally to this work. The authors gratefully acknowledge the assistance of Thitiporn Sukaew, Gustavo Serrano, Forest Bohrer, Katharine Beach, Brendan Casey, Robert Gordenker, and Brad Richert from the University

of Michigan; David Burris and Jim Reisinger from Integrated Science and Technology, Inc. (IST, Inc.); and Kyle Gorder from Hill Air Force Base. This work was supported by DoD ESTCP Grant ER-200702 through a subcontract with IST, Inc., and by the Engineering Research Centers Program of the National Science Foundation under Award Number ERC-9986866. Devices described in this report were fabricated in the Lurie Nanofabrication Facility, a member of the National Nanotechnology Infrastructure Network, which is supported by the National Science Foundation.

REFERENCES

(1) Kim, H.; Astle, A.; Najafi, K.; Bernal, L. P.; Washabaugh, P. D. Tech. Digest 20th *IEEE International Conf. Microelectromechanical System (MEMS)*, Kobe, Japan, January 21−25, 2007; pp 131−134.

(2) (a) Kim, M.; Mitra, S. *J. Chromatogr.* **2003**, *996*, 1–11. (b) Tian, W. C.; Pang, S. W.; Lu, C. J.; Zellers, E. T. *J. Microelectromech. Syst.* **2003**, *12*, 264–272. (c) Tian, W. C.; Chan, K. L. H.; Lu, C.-J.; Pang, S. W.; Zellers, E. T. *J. Microelectromech. Syst.* **2005**, *14*, 498–507. (d) Voiculescu, I.; McGill, R. A.; Zaghloul, M. E.; Mott, D.; Stepnowski, J.; Stepnowski, S.; Summers, H.; Nguyen, V.; Ross, S.; Walsh, K.; Martin, M. *IEEE Sens. J.* **2006**, *6*, 1094–1104. (e) Camara, E. H. M.; Breuil, P.; Briand, D.; Guillot, L.; Pijolat, C.; de Rooij, N. F. *Sens. Actuators, B* **2010**, *148*, 610–619. (f) Manginell, R. P.; Adkins, D. R.; Moorman, M. W.; Hadizadeh, R.; Copic, D.; Porter, D. A.; Anderson, J. M.; Hietala, V. M.; Bryan, J. R.; Wheeler, D. R.; Pfeifer, K. B.; Rumpf, A. *J. Microelectromech. Syst.* **2008**, *17*, 1396–1407. (g) Veeneman, R. A.; Zellers, E. T. *Tech. Digest Solid-State Sensor, Actuator, Microsystems Workshop,* Hilton Head, SC, June 1−5, 2008; pp 252−255. (h) Manginell, R. P.; Lewis, P.; Adkins, D. R.; Wheeler, D. R.; Simonson, R. J. U. S. Patent 7,799,280, September 21, 2010.

(3) (a) Noh, H.; Hesketh, P. J.; Frye-Mason, G. C. *J. Microelectromech. Syst.* **2002**, *11*, 718–725. (b) Dziuban, J. A.; Mroz, J.; Szczygielska, M.; Malachowski, M.; Gorecka-Drzazga, A.; Walczak, R.; Bula, W.; Zalewski, D.; Nieradko, L.; Lysko, J.; Koszur, J.; Kowalski, P. *Sens. Actuators, A* **2004**, *115*, 318–330. (c) Lambertus, G.; Elstro, A.; Sensenig, K.; Potkay, J.; Agah, M.; Scheuering, S.; Wise, K.; Dorman, F.; Sacks, R. *Anal. Chem.* **2004**, *76*, 2629–2637. (d) Agah, M.; Potkay, J. A.; Lambertus, G.; Sacks, R.; Wise, K. D. *J. Microelectromech. Syst.* **2005**, *14*, 1039–1050. (e) Bhushan, A.; Yemane, D.; Trudell, D.; Overton, E. B.; Goettert, J. *Microsyst. Technol.* **2007**, *13*, 361–368. (f) Reidy, S.; Lambertus, G.; Reece, J.; Sacks, R. *Anal. Chem.* **2006**, *78*, 2623–2630. (g) Stadermann, M.; McBrady, A. D.; Dick, B.; Reid, V. R.; Noy, A.; Synovec, R. E.; Bakajin, O. *Anal. Chem.* **2006**, *78*, 5639–5644. (h) Potkay, J. A.; Lambertus, G. R.; Sacks, R. D.; Wise, K. D. *J. Microelectromech. Syst.* **2007**, *16*, 1071–1079. (i) Radadia, A. D.; Masel, R. I.; Shannon, M. A.; Jerrell, J. P.; Cadwallader, K. R. *Anal. Chem.* **2008**, *80*, 4087–4094. (j) Ali, S.; Ashraf-Khorassani, M.; Taylor, L. T.; Agah, M. *Sens. Actuators, B* **2009**, *141*, 309–315. (k) Kim, S. K.; Chang, H.; Zellers, E. T. *Tech. Digest Transducers '09*, Denver, CO, June 21−25, 2009, pp 128−131. (l) Serrano, G.; Reidy, S. M.; Zellers, E. T. *Sens. Actuators, B* **2009**, *141*, 217–226. (m) Frye-Mason, G.; Kottenstette, R.; Lewis, P.; Heller, E.; Manginell, R.; Adkins, D.; Dulleck, G.; Martinez, D.; Sasaki, D.; Mowry, C.; Matzke, C.; Anderson, L. *Proceedings of Micro Total Analysis Systems (μTAS) Workshop*, Enschede, Netherlands, May 14−18, 2000, pp 229−232.

(4) (a) Cai, Q.-Y.; Zellers, E. T. *Anal. Chem.* **2002**, *74*, 3533–3539. (b) Lu, C.-J.; Whiting, J.; Sacks, R. D.; Zellers, E. T. *Anal. Chem.* **2003**, *75*, 1400–1409. (c) Steinecker, W. H.; Rowe, M.; Matzger, A.; Zellers, E. T. *Tech. Digest Transducers '03*, Boston, MA, June 9−13, 2003, pp 1343−1346. (d) Hsieh, M.-D.; Zellers, E. T. *Anal. Chem.* **2004**, *76*, 1885–1895. (e) Archibald, R.; Datskos, P.; Devault, G.; Lamberti, V.; Lavrik, N.; Noid, D.; Sepaniak, M.; Dutta, P. *Anal. Chim. Acta* **2007**, *584*, 101–105. (f) Steinecker, W. H.; Rowe, M. P.; Zellers, E. T. *Anal. Chem.* **2007**, *79*, 4977–4986. (g) Jin, C.; Kurzawski, P.; Hierlemann, A.; Zellers, E. T. *Anal. Chem.* **2008**, *80*, 227–236. (h) Jin, C.; Zellers, E. T. *Anal. Chem.* **2008**, *80*, 7283–7293. (i) Jin, C.; Zellers, E. T. *Sens. Actuators, B* **2009**, *139*, 548–556. (j) Rairigh, D. J.; Warnell, G. A.; Xu, C.; Zellers, E. T.; Mason, A. J. *IEEE Trans. Biomed. Circuits Syst.* **2009**, *3*, 267–276. (k) Zhong, Q.; Steinecker, W. H.; Zellers, E. T. *Analyst* **2009**, *134*, 283–293. (l) Covington, E.; Bohrer, F. I.; Xu, C.; Zellers, E. T.; Kurdak, Ç. *Lab Chip* **2010**, *10*, 3058–3060. (m) Li, M.; Myers, E. B.; Tang, H. X.; Aldridge, S. J.; McCaig, H. C.; Whiting, J. J.; Simonson, R. J.; Lewis, N. S.; Roukes, M. L. *Nano Lett.* **2010**, *10*, 3899–3903. (n) Bohrer, F. I.; Covington, E.; Kurdak, Ç.; Zellers, E. T. *Anal. Chem.* **2011**, *83* (10), 3687–3695. (o) Steinecker, W. H.; Kim, S. K.; Bohrer, F. I.; Farina, L.; Kurdak, Ç.; Zellers, E. T. *IEEE Sens. J.* **2011**, *11*, 469–480. (p) Lu, C. J.; Jin, C.; Zellers, E. T. *J. Environ. Monit.* **2006**, *8*, 270–278. (q) Zhong, Q.; Veeneman, R. A.; Steinecker, W. H.; Jia, C.; Batterman, S. A.; Zellers, E. T. *J. Environ. Monit.* **2007**, *9*, 440–448.

(5) Lambertus, G. R.; Fix, C. S.; Reidy, S. M.; Miller, R. A.; Wheeler, D.; Nazarov, E.; Sacks, R. *Anal. Chem.* **2005**, *77*, 7563–7571.

(6) Serrano, G.; Chang, H.; Zellers, E. T. *Tech. Digest Transducers '09*, Denver, CO, June 21−25, 2009, pp 1654−1657.

(7) (a) Lu, C.-J.; Tian, W.-C.; Steinecker, W. H.; Guyon, A.; Agah, M.; Oborny, M. C.; Sacks, R.; Wise, K. D.; Pang, S. W.; Zellers, E. T. *Proc. 7th International Conference on Miniaturized Chemical and Biochemical Analysis Systems (μTAS '03):* Squaw Valley, CA, October 5−9, 2003, pp 415−419. (b) Zellers, E. T.; Steinecker, W. H.; Lambertus, G.; Agah, M.; Lu, C.-J.; Chan, H. K. L.; Potkay, J. A.; Oborny, M. C.; Nichols, J. M.; Astle, A.; Kim, H. S.; Rowe, M.; Kim, J.; da Silva, L. W.; Zheng, J.; Whiting, J. *Tech. Digest Solid-State Sensors, Actuator and Microsystems Workshop*, Hilton Head, SC, June 6−10, 2004, pp 61−66. (c) Lu, C.-J.; Steinecker, W. H.; Tian, W.-C.; Oborny, M. C.; Nichols, J. M.; Agah, M.; Potkay, J. A.; Chan, H. K. L.; Driscoll, J.; Sacks, R. D.; Wise, K. D.; Pang, S. W.; Zellers, E. T. *Lab Chip* **2005**, *5*, 1123–1131. (d) Lewis, P. R.; Manginell, R. P.; Adkins, D. R.; Kottenstette, R. J.; Wheeler, D.; Sokolowski, S. S.; Trudell, D.; Byrnes, J. E.; Okandan, M.; Bauer, J. M.; Manley, R. G.; Frye-Mason, C. *IEEE Sens. J.* **2006**, *6*, 784–795. (e) Kim, H.; Steinecker, W. H.; Reidy, S.; Lambertus, G. R.; Astle, A. A.; Najafi, K.; Zellers, E. T.; Bernal, L. P.; Washabaugh, P. D.; Wise, K. D. *Tech. Digest Transducers '07*, Lyon, France, June 10−14, 2007, pp 1505−1508. (f) Zellers, E. T.; Reidy, S.; Veeneman, R. A.; Gordenker, R.; Steinecker, W. H.; Lambertus, G. R.; Kim, H.; Potkay, J. A.; Rowe, M. P.; Zhong, Q.; Avery, C.; Chan, H. K. L.; Sacks, R. D.; Najafi, K.; Wise, K. D. *Tech. Digest Transducers '07*, Lyon, France, June 10−14, 2007, pp 1491−1494. (g) Zampolli, S.; Elmi, I.; Mancarella, F.; Betti, P.; Dalcanale, E.; Cardinali, G. C.; Severi, M. *Sens. Actuators, B* **2009**, *141*, 322–328. (h) Chang, H.; Kim, S. K.; Sukaew, T.; Bohrer, F.; Zellers, E. T. *Tech. Digest Solid-State Sensors, Actuator and Microsystems Workshop,* Hilton Head, SC, June 6−10, 2010, pp 278−281. (i) Chang, H.; Kim, S. K.; Sukaew, T.; Bohrer, F.; Zellers, E. T. *Procedia Eng.* **2010**, *5*, 973–976. (j) http://www.defiant-tech.com. (Accessed August, 2011).

(8) http://www.wimserc.org/. (Accessed August, 2011).

(9) Beach, K. T.; Reidy, S.; Gordenker, R. J.; Wise, K. D. *Tech. Digest 24th IEEE International Conf. Microelectromechanical Systems (MEMS)*, Cancun, Mexico, January 23−27, 2011, pp 813−816.

(10) Sukaew, T.; Chang, H.; Serrano, G.; Zellers, E. T. *Analyst* **2011**, *136*, 1664–1674.

(11) Wallner, J. Z.; Hunt, K. S.; Obanionwu, H.; Oborny, M. C.; Bergstrom, P. L.; Zellers, E. T. *Phys. Status Solidi A* **2007**, *204*, 1449–1453.

(12) Kim, S.-J.; Reidy, S. M.; Block, B. P.; Wise, K. D.; Zellers, E. T.; Kurabayashi, K. *Lab Chip* **2010**, *10*, 1647–1654.

(13) Kim, S.-J.; Serrano, G.; Wise, K. D.; Kurabayashi, K.; Zellers, E. T. *Anal. Chem.* **2011**, *83*, 5556–5562.

(14) Seo, J. H.; Kim, S. K.; Zellers, E. T.; Kurabayashi, K. *Tech. Digest 24th IEEE International Conf. Microelectromechanical Systems (MEMS)*, Cancun, Mexico, January 23−27, 2011, pp 825−828.

(15) Kim, S. K.; Chang, H.; Bryant, J. G.; Burris, D. R.; Zellers, E. T. *Tech. Digest Transducers '11*, Beijing, China, June 5−9, 2011, pp 799−802.

(16) Zellers, E. T.; Serrano, G.; Chang, H.; Amos, L. K. *Tech. Digest Transducers '11*, Beijing, China, June 5−9, 2011, pp 2082−2085.

(17) U. S. EPA. *Draft Guidance for Evaluating the Vapor Intrusion to Indoor Air Pathway from Groundwater and Soils*; U. S. EPA: Washington, DC, 2002, available at http://www.epa.gov/osw/hazard/correctiveaction/eis/vapor/complete.pdf.

(18) Chiu, W. A.; Caldwell, J. C.; Keshava, N.; Scott, C. S. *Environ. Health Perspect.* **2006**, *114*, 1445–1449.
(19) Fitzpatrick, N. A.; Fitzgerald, J. J. *Proceedings of the 11th Annual Conference on Contaminated Soils*, Amherst, MA, October 21−24, 1996, pp 1−15.
(20) ATSDR. *Public Health Assessment:* Hill Air Force Base, Utah, Davis and Weber Counties, Utah, Federal Facilities Assessment Branch, Division of Health Assessment and Consultation, ATSDR, 2003, available at http://www.atsdr.cdc.gov/hac/pha/pha.asp?docid=795&pg=0, accessed June 2011.
(21) Folkes, D.; Wertz, W.; Kurtz, J.; Kuehster, T. *Ground Water Monit. Rem.* **2009**, *29*, 70–80.
(22) McHugh, T.; Connor, J.; Ahmad, F. *Environ. Forensics* **2004**, *5*, 33–44.
(23) Inficon, *Hapsite*, available at http://www.inficonchemicalidentificationsystems.com, accessed June 2011.
(24) Fair, J. D.; Bailey, W. F.; Felty, R. A.; Gifford, A. E.; Shultes, B.; Volles, L. H. *J. Environ. Sci.* **2009**, *21*, 1005–1008.
(25) U. S. Air Force (AFIOH), *Guide for the Assessment of the Vapor Intrusion Pathway*, U.S. Air Force, 2006; available at http://airforcemedicine.afms.mil/idc/groups/public/documents/afms/ctb_050032.pdf.
(26) Lu, C. J.; Zellers, E. T. *Analyst* **2002**, *127*, 1061–1068.
(27) Rowe, M. P.; Plass, K. E.; Kim, K.; Kurdak, Ç.; Zellers, E. T.; Matzger, A. *Chem. Mater.* **2004**, *16*, 3513–3517.
(28) U. S. Environmental Protection Agency (EPA). *Compendium Method TO-15*, Second ed.; U.S. Environmental Protection Agency, 1996, available at http://www.epa.gov/ttnamti1/files/ambient/airtox/to-15r.pdf